

Studies of Mode Lock Instability in the HL-1M Tokamak

Qingwei Yang, Longwen Yan, and Jun Qian
Southwestern Institute of Physics, Chengdu, Sichuan 610041, China

Received on 26 June, 2001

Locked mode instability in the HL-1M tokamak has been investigated in this paper. In the HL-1M tokamak the mode lock instability often appears in with low density discharges ($\bar{n}_e < 1 \times 10^{19} \text{ m}^{-3}$). The precursor perturbations on both soft-X rays and Mirnov signals simultaneously increase before mode locking. Their frequencies are the same and gradually decrease, which indicate that the perturbation is global. Their existence time-scale is about 10ms. The plasma will suddenly stop rotating when the fluctuation amplitude or frequency reaches a threshold. Mode lock instability can often cause major disruptions. The rotation frequency is decreased to about 3kHz before mode locking in the HL-1M tokamak, which is consistent with the theoretical model.

I Introduction

Major disruptions in plasmas are dangerous not only for present tokamaks but also for future reactors. It is important to study the mechanism of major disruption, and try to avoid it. A few kinds of major disruption, such as the displacement disruption, density limited disruption, low q_a disruption and β limit disruption have been observed in tokamak experiments. They always are connected with the MHD instabilities. In this paper, the major disruption caused by the mode lock instability has been studied. The frequencies of the mode rotation gradually slow down while the MHD instabilities grow up, and then mode lock appears when the rotation stops suddenly. The mode lock instability can be observed at current ramp up, plateau and ramp down phases. In particularly, it is easy to appear in low-density discharges.

The experimental results on JET tokamak [1] showed that major disruptions caused by the mode lock instability often appeared when the electron density was lower than a threshold. The threshold is dependent on the plasma parameters. For example, the threshold will decrease in the experiments with neutral beam injection. The error field instability is the main reason

of mode lock instability. A small asymmetrical magnetic field can lead up to the development of error field instability. In D III - D tokamak [2], the mode lock instability was observed with precursor perturbations before the low density or the density limit disruptions. The locked mode may appear at one or several toroidal places. The mode lock instability could be enhanced or suppressed by an additional $n = 1$ magnetic field. The variety of the stable operation region depends whether the error field is increased or decreased. The experiments of JT-60U tokamak [3] indicated that the error field instability was observed with the large elongation ratio ($k = b/a > 1.5$). In the neutral beam injection (NBI) experiment, the error field instability was suppressed. The experiments of COMPASS-C tokamak [4] indicated that the error field instability is not a serious problem in small size tokamaks.

II Theoretical model

To use the nonlinear tearing mode theory and consider the interaction between rotated plasma and static resonant magnetic perturbation, Fitzpatrick gave the equation about the critical amplitude of radial magnetic perturbation as follow [5]:

$$\frac{B_{r,mn}}{B_t} \Big|_{r=a} \approx 6.7[g^2] \left[\left(\frac{r_s}{a} \right)^{2-m} \left(\frac{q^2 r_s}{m^4 R_0} \right)^{1/3} \left(\frac{-\Delta'_0 r_s}{S_B} \right)^{1/3} \right] [(f\tau_A)^{4/3}] \quad (1)$$

where m and n are the mode numbers at the rational surface $r_s(q(r_s) = m/n)$. The factor g in the first parenthesis is weakly dependent on viscosity. The term in the second parenthesis is the function of current profile and the MHD mode. Here $-\Delta'_0 r_s$ is the non-dimensional parameter of tearing mode, and $S_B = \frac{r}{a} \frac{dq}{dr}$ is the factor of magnetic shear. The parameters f and τ_A in the third parenthesis are the frequency of plasma rotation and the Alfvén time, respectively. Taking $\tau_A \equiv R_0(\mu_0 \bar{n} m_i)^{1/2} / B_t$, m_i being the mass of ion, we can obtain the following equation for considering the 2/1 mode:

$$\left. \frac{B_{r21}}{B_t} \right|_{r=a} \sim \left(\frac{fR}{B_t} \right)^{4/3} \bar{n}^{2/3} \quad (2)$$

For the COMPASS-C and D III-D tokamaks, the calculated values from formula (2) are consistent with the experimental results. To increase the frequency of plasma rotation, we can obtain the higher threshold value of the magnetic perturbation.

For Ohmic heated plasmas, the rotation frequency of magnetic perturbation is about the electron drift frequency f_{De} :

$$f \approx f_{De} \propto \frac{kT_{e0}}{eB_t a^2} \quad (3)$$

Here, k is the Boltzmann constant and T_{e0} is the central electron temperature. For the COMPASS-C device, $T_{e0} \sim 600\text{eV}$, $B_t = 1.1\text{T}$, $R=0.56\text{m}$, $a=0.18\text{m}$, the calculated electron drift frequency is $f_{De} \sim 15\text{kHz}$, and the experimental result is $f=13\text{kHz}$. For the D III - D tokamak, $T_{e0} \sim 920\text{eV}$, $B_t = 1.3\text{T}$, $R=1.67\text{m}$, $a=0.67\text{m}$, $f_{De} \sim 1.7\text{kHz}$ and the experimental result is $f=1.6\text{kHz}$. For the HL-1M tokamak, $T_{e0} \sim 700\text{eV}$, $B_t = 2.1\text{T}$, $R=1.02\text{m}$, $a=0.26\text{m}$, $f_{De} \sim 3.2\text{kHz}$ and the experimental result is $f = 3.1\text{kHz}$. The theoretic predictions are, therefore, very consistent with the experiment results.

Supposing that the safe factor q_a and the $\epsilon = a/R$ are constant, the following formula can be obtained by using Pfeiffer-Waltz energy confinement scaling [6].

$$f \approx f_{De} \sim R_0^{-9/5} B_t^{-1/5} \quad (4)$$

Combined with the Murakami scaling $\bar{n} \sim B_t/R_0$, the scaling formula is given by:

$$\left. \frac{B_{r21}}{B_t} \right|_{r=a} \sim R_0^{-26/15} B_t^{-14/15} \quad (5)$$

The threshold value of $m/n = 2/1$ mode perturbation is approximately inverse of the square of major radius R and toroidal field B_t of tokamaks. Thus, the mode lock instability, caused by error field, will be a serious problem on large size tokamak.

III Experimental results

HL-1M tokamak is a middle size device. Its major radius is 102cm, minor radius is 26cm, toroidal field is 2.8T, plasma current is 320kA, and discharge duration can reach up to 4.0 s. Fast vertical and radial field feedback systems are used to control the plasma displacement. The plasma current is controlled by feedback as well. The mode lock instability are sometimes observed during the HL-1M tokamak discharges, but the sources of the error field have not been calculated accurately.

During the HL-1M experiments, the Mirnov coils and the soft X-ray arrays are used to diagnose the magnetohydrodynamical (MHD) instabilities. 32 Mirnov coils are uniformly distributed in the poloidal direction at one toroidal section. The coil located at higher magnetic field side is named No.01, and at lower field side is No.16. 16 of them are used for studying the MHD perturbations and are sampled at the sampling rate of 20kbs. The signal from the inside coil is MIR01, and that from the outside one is MIR08. The integrated signals from SMIR01 to SMIR32, picked up from all the 32 coils, are measured at the sampling rate of 2kbs. 3 arrays of soft X-ray detectors are used to detect the MHD perturbations at the plasma central region and to make tomography analysis. Other diagnostic instruments, including HCN laser interferometer, bolometer and Langmuir probes, are used to measure the plasma density, plasma emission, edge density and temperature, respectively.

Typically, the mode lock instability appears during the low density experiments. In shot 6201, for example, the plasma current is $I_p = 135\text{kA}$, the toroidal field is $B_t=2.1\text{T}$, and the line-average electron density is $\bar{n}_e = 0.7 \times 10^{19}\text{m}^{-3}$, as shown in Fig. 1. Before the MHD instability is observed, the edge electron temperature drops down from 40eV to a few electron-volts, and the edge electron density increases. The rotation frequency slows down gradually from 5kHz to 3.1kHz, while the amplitude of the perturbation grows up. The mode lock instability appears after the MHD instability has developed for about 40ms. This MHD instability has also been observed at the central, channel soft X-ray which indicates that this perturbation is a global one. In this shot, the plasma current was not quenched by the disruption. This is because of the low density and the fast feedback control of plasma current. To observe the mode lock disruption in detail, the signals from 131ms to 139ms are shown in Fig. 2. After the mode lock instability has been triggered, in 2ms, a positive spike is observed on the central channel soft X-ray signal, within the time-scale of 0.2ms, and then the

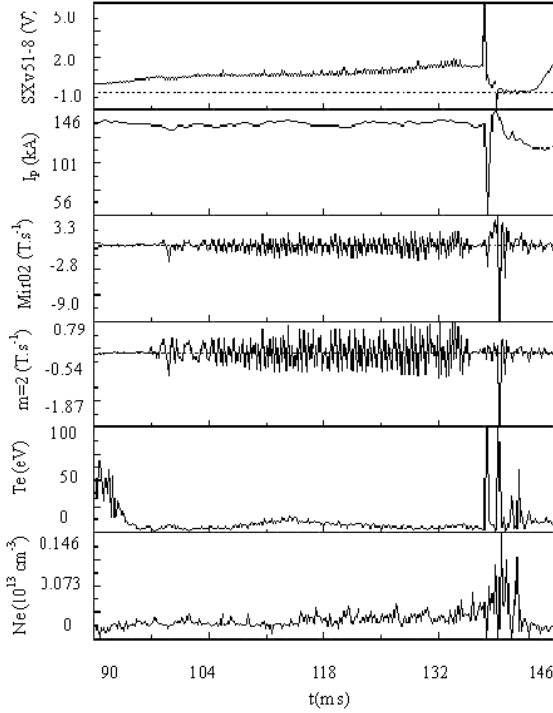


Figure 1. The evolution of the mode lock instability that occurred in shot 6201. The waveforms from top to bottom are: intensity of central channel soft X-rays, plasma current, Mirnov perturbation at higher field side, perturbation of the $m=2$ mode, electron temperature and the electron density at $r/a = 1.02$, respectively.

disruption takes place at 137ms. The positive spike indicates that the parallel energy of suprathermal electrons changes into perpendicular when the instability in the velocity-space occurs, and the energy is rapidly lost. Then the intensity of the soft X-ray decreases while the energy of thermal electrons is lost. The disruption makes the plasma current drops down to about 15%. On the other hand, the poloidal magnetic field at lower field side increases, while it decreases in the higher field side. A mode is locked at the lower field side, which is the typical phenomenon of the mode lock instability. During the disruption appearance, the plasma edge electron temperature and density undergo great changes. The electron temperature rises rapidly, which corresponds to electrons that lose their energy within the time-scale of about 0.1ms. After ~ 0.3 ms, the edge temperature drops down to the original level and the edge density increases. This indicates that the energy loss ended and the particle loss started. The plasma stored energy and particles are rapidly lost within 1ms, but energy loss is faster than the particle one.

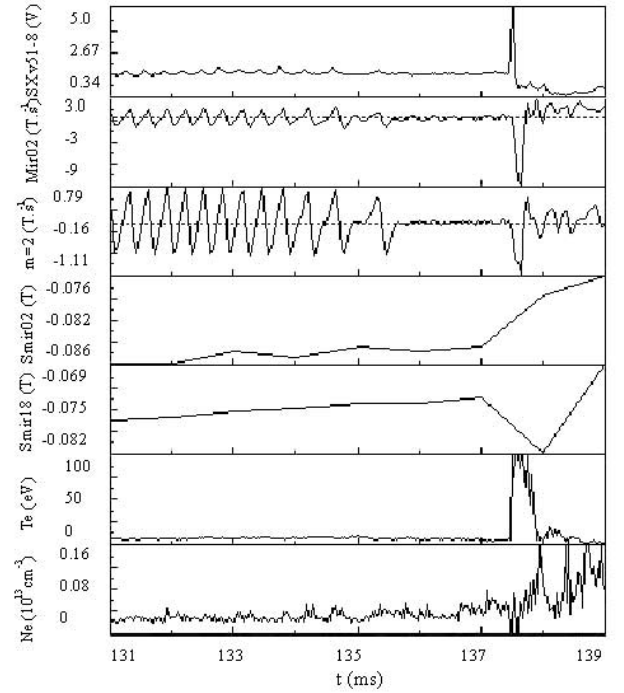


Figure 2. Temporal extension of mode lock on shot 6201. The waveforms from top to bottom are the intensity of central channel soft X-rays, the Mirnov perturbation at higher field side, the perturbation of $m=2$ mode, the negative signal of poloidal field at higher field side, the negative signal of poloidal field at lower field side, the electron temperature and the electron density at $r/a = 1.02$, respectively.

Another discharge with mode lock instability of low density is given in Fig. 3. In this shot, the plasma current is $I_p=135$ kA, toroidal field is $B_t=2.1$ T, and the line-average electron density is $\bar{n}_e = 0.4 \times 10^{19} \text{m}^{-3}$, respectively. During the existence of MHD activity (137ms-143ms), the instability caused two small positive spikes to appear in the central channel soft X-ray signal. Fig. 4 gives the detail of these waveforms related to the mode lock instability that takes place from 136ms to 152ms. A small positive spike is found at 138ms, and then the $m=2$ mode grows up. After ~ 5 ms, the mode lock appears. A big positive spike is observed on soft X-ray before the disruption occurrence. The edge electron temperature rapidly increased during mode lock appearance. After several milliseconds, also the edge electron density increases subsequently, which indicates that the energy loss is faster than the particle one.

For comparing the mode lock instability with the normal MHD instabilities, typical diagnostic waveforms corresponding to high density discharges are given in Fig. 5. In this shot, the plasma current is $I_p=150$ kA,

the toroidal field is $B_t=2.0\text{T}$ and the line-average electron density is $\bar{n}_e = 7.0 \times 10^{19}\text{m}^{-3}$, respectively. The edge temperature continuously drops and the edge density gradually increases with the rise of the electron density. The precursor oscillation appears at about 270ms. Major disruption takes place after a few minor disruptions. Finally, the discharge is suddenly stopped. The positive spikes on soft X-rays and locked mode have not been observed during high density disruption, which reveals that the suprathermal electrons are very low at high density discharges. For the discharges with high density, the MHD mode cannot be locked before the minor disruptions, as shown in Fig. 6. After the last minor disruptions, the edge temperature rises. It indicates that much of the stored energy is lost through the plasma edge. It is difference from that in mode locking discharges.

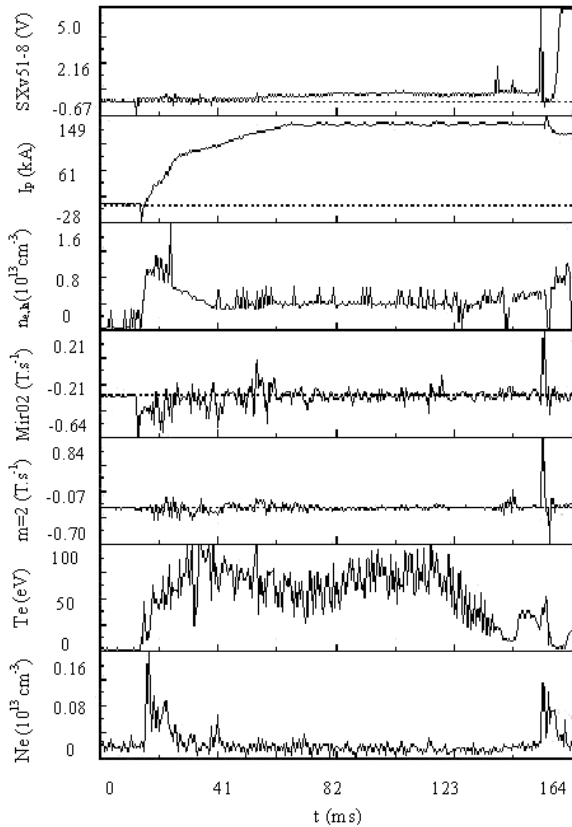


Figure 3. The evolution of the mode lock instability that occurred in shot 6211. The waveforms from top to bottom are the intensity of central channel soft X-ray, plasma current, line-average electron density, the Mirnov perturbation at higher field side, perturbation of $m=2$ mode, electron temperature and electron density at $r/a = 0.98$, respectively.

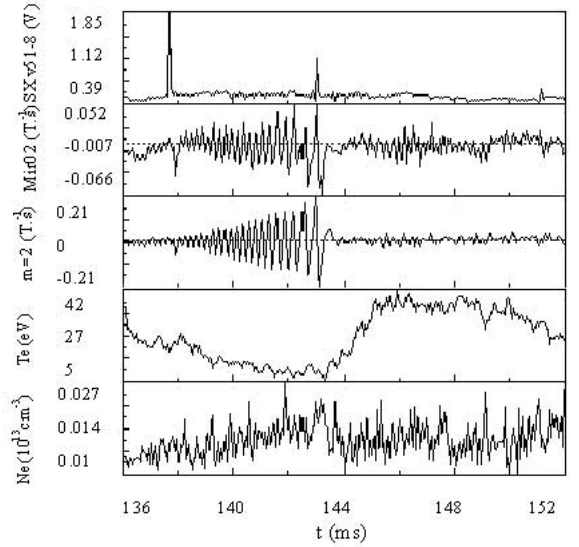


Figure 4. Temporal extension of mode lock on shot 6211. The waveforms from top to bottom are the intensity of central channel soft X-rays, the Mirnov perturbation at higher field side, the perturbation of $m = 2$ mode, the electron temperature and the electron density at $r/a = 0.98$, respectively.

IV Conclusion

Mode lock instability on the HL-1M tokamak has been investigated in this paper. The precursor perturbations between mode lock instability and high-density disruption are compared. Locked mode instability often appears in very low density discharges ($\bar{n}_e < 1 \times 10^{19}\text{m}^{-3}$). Magnetic perturbations on both soft-X rays and Mirnov signals simultaneously increase before mode locking. Their frequencies are the same and gradually decrease, indicating that the perturbation is a global one. The corresponding time-scale is about 10ms.

The rotation frequency is decreased to about 3kHz before mode locking in the HL-1M tokamak, which is consistent with the predication of theoretic model. Major disruption takes place after locked mode appears, within a few milliseconds. Plasma stored energy and particles are rapidly lost within 1ms, but energy loss is faster than the particle one. A sharp positive spike on central channel soft X-rays and current has been ob-

served within the time-scale of 0.2ms during major disruption, which shows that the suprathreshold electrons are lost faster than the thermal ones. The poloidal magnetic field at inside drops, while it increases outside, which represents that the MHD instability appears mainly at lower side of the magnetic field.

The best way to suppress the mode locking instability is to decrease the inherece error field in tokamaks and to increase the plasma density.

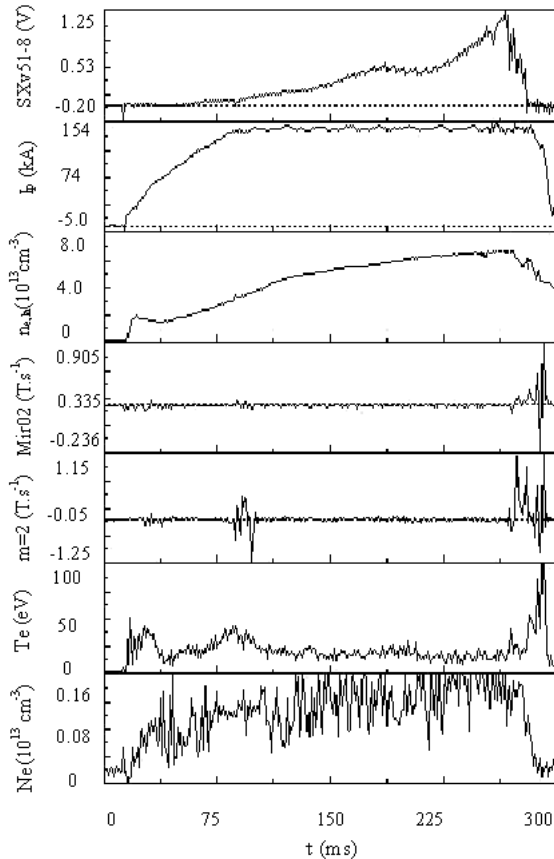


Figure 5. A typical disruption with high density for shot 6079. The waveforms from top to bottom are the intensity of central channel soft X-rays, the plasma current, the line-average electron density, the Mirnov perturbation at higher field side, the perturbation of $m = 2$ mode, the electron temperature and the electron density at $r/a = 0.98$, respectively.

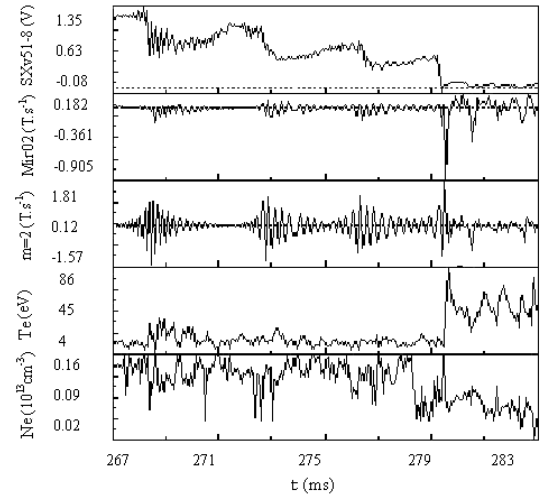


Figure 6. Temporal extension of high-density disruption for shot 6079. The waveforms from top to bottom are the intensity of central channel soft X-rays, the Mirnov perturbation at higher field side, the perturbation of $m = 2$ mode, the electron temperature and the electron density at $r/a = 0.98$, respectively.

Acknowledgement

This research is partially supported by National Science Foundation of China under grant of No. 19889504.

References

- [1] G.M. Fishpool and P.S. Haynes, Nucl. Fusion **38**, 109 (1994).
- [2] J.T. Scoville, R.J. La Haye, A.G. Kellman, et. al. Nucl. Fusion **31**, 875 (1991).
- [3] R. Yoshino, Y. Nayatani, N. Isei *et al.* Journal of Plasma and Fusion Research **10**, 1081 (1994).
- [4] R.J. La Haye, R. Fitzpatrick, T.C. Hender, *et al.* Phys. Fluids B**4**, 2096 (1992).
- [5] R. Fitzpatrick and T.C. Hender, Phys. Fluids B**3**, 644 (1991).
- [6] W.W. Pfeiffer and R.E. Waltz, Nucl. Fusion **19**, 51 (1979).